Journal of Thermal Engineering
Yildiz Technical University Press, Istanbul, Turkey
Vol. 2, No. 1, pp. 566-574, January, 2016.

http://eds.yildiz.edu.tr/journal-of-thermal-engineering/Articles
Manuscript Received April 13, 2015; Accepted July 13, 2015

This paper was recommended for publication in revised form by Editor in Chief Ahmet Selim Dalkilic

PRESTRESSED STAYED CROSSARMED WIND TURBINE TOWERS

Jack Callaghan
Northumbria University
Newcastle upon Tyne, UK

***Alireza Maheri**
Northumbria University
Newcastle upon Tyne, UK

Keywords: wind turbine tower, cross-armed columns, stayed column, buckling, tower design
** Corresponding author:* Alireza Maheri
Phone: +44 (0) 191 227 3860
E-mail address: Alireza.Maheri@northumbria.ac.uk

ABSTRACT

One of the major components of horizontal axis wind turbines is the tower, which supports the weight of the rotor and nacelle as well as the thrust force produced by the rotor. Wind turbine towers are designed for static stability under the axial load, for strength to withstand the cantilever thrust force and for dynamic stability in interaction with rotating rotor and blades. This paper presents the results of a numerical investigation into an innovative wind turbine tower design, using the concept of pre-stressed stayed cross-armed columns. Pre-stressed stayed cross-armed columns restrain the column buckling deformation as a result of the tension in the cables causing compression in the horizontal cross-arms. This essentially decreases the effective length of the column, thereby giving it superior axial load resistance against buckling.

INTRODUCTION

A wind turbine tower supports the head assembly and facilitates the transfer of generated power to ground level. Towers are designed to be strong enough to resist buckling under the axial load of the head assembly and stiff enough to withstand deformation from the cantilever forces generated by the wind in the form of thrust acting on the rotor. They are also mechanically sound in various other conditions such as eccentric loading and wind loading, following standards IEC 61400-1, EN 1993-1-1, and IS0 2394. Fig. 1 shows the basic forces acting on a wind turbine tower, the wind and head assembly loads and moment due to rotor thrust [1].

The Wind Profile Power Law dictates that wind speed increases proportionally to the seventh root of altitude, meaning a tower twice as tall is subjected to 10% higher wind speed and 34% increased power. Another wind condition taken into account is Extreme Operating Gust (EOG). This is when a sudden increase in wind speed causes a distributed impact load on the wind turbine causing a vibration. The magnitude of the gust is numerically calculated. These conditions mean that as wind turbines increase in size and power generation, the towers need to be taller and have proportionately higher force resisting characteristics, to enable this growth and compensate for more violent environmental conditions.

Larger towers can provide challenges in transport, erection, and subsequently the total cost of such structures. The cost of a tower is 20-30% of the total for a wind turbine, and transport is estimated to be another 10-15% on top of that [2]. Across the EU the maximum width allowed for a lorry is 2.55-2.6m, the maximum length is 12-24m, and the maximum height is 4-4.2m [3]. If the same design of wind turbine tower that is currently used is retained in the future, transportation difficulties will arise, as in some countries the maximum transportable width is 4.9m, and it is estimated wind turbine tower diameters would approach 5m.

During wind turbine tower erection, the larger and heavier the parts are, the more specialised and higher duty rated the lifting equipment needs to be, thereby increasing costs of rental and operation.

The most widely used tower type for large wind turbines is the freestanding tubular steel tower. These comprise of multiple conical sections that are welded from bended steel plates off-site, and assembled on-site by means of welding or flanged mechanical fixing. The base section is secured to the foundations by mechanical fixation to the anchor bolts. Tubular towers have limited wall thickness, dictated by steel plate bending manufacturing limits. Other types of wind turbine towers include guyed, guyed tilt-up, multiple legged, freestanding lattice, concrete, floating, and hybrid.

This paper aims at investigating the suitability of the concept of pre-stressed stayed columns, originally developed and investigated for tall columns [4-10], for multi-MW wind turbine towers.

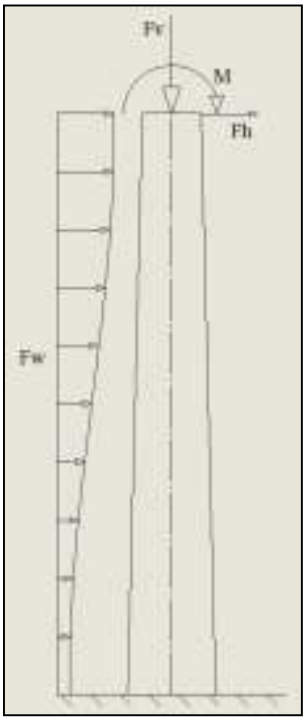

FIGURE 1-BASIC FORCES ON WIND TURBINE TOWER

PRESTRESSED STAYED COLUMNS

Ordinary, non-stayed columns tend to be slender, which means they are susceptible to buckling under axial load. Prestressed stayed columns restrain the column buckling deformation as a result of the tensioned cables causing compression in the horizontal crossarms which acts perpendicularly on the column at the midpoint. This essentially decreases the effective length of the column, thereby giving it superior axial load resistance against buckling [4].

Buckling of a prestressed stayed column is analysed theoretically in reference to the dimensions shown in Fig. 2 [5]. The equations are derived from [6]. The stiffness of the system components are calculated using subscript c, a, and s for the column, crossarms and stays respectively where

$$K_x = \frac{E_x A_x}{L_x} \qquad (1)$$

and is used to find the value C_{11} , where

$$C_{11} = \frac{\cos(\alpha)}{2\left[\frac{K_c}{K_s} + \frac{2K_c(\sin^2\alpha)}{K_a} + \cos^2\alpha\right]} \qquad (2)$$

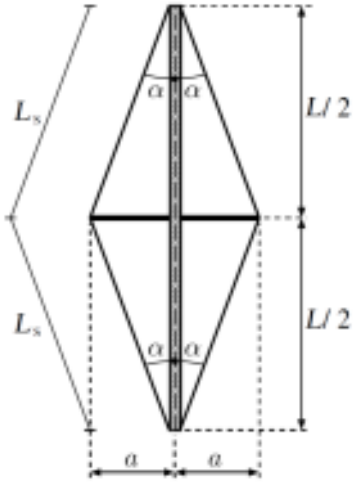

FIGURE 2-CROSSAREMED COLUMN [5]

The critical buckling load for the non-stayed column is determined using

$$N_{cr} = \frac{\pi^2 EI}{{L_e}^2} \qquad (3)$$

Hence the minimum effectual stay tension for the system for the symmetric and antisymmetric eigenmodes is calculated

$$T_{min,sym} = C_{11} N_{cr} \qquad (4)$$

$$T_{min,anti} = 4C_{11} N_{cr} \qquad (5)$$

Whether or not the failure mode is symmetric or antisymmetric is determined by comparing the stayed column maximum critical buckling load (N^c_{max}) for each eigenmode. The smaller value of the two is the failure mode, and the T_{min} can be taken derived from the same mode where

$$N^c_{max,sym} = \frac{4{D_{sym}}^2 E_c I_c}{{L_c}^2} \qquad (6)$$

$$N^c_{max,anti} = \frac{4{D_{anti}}^2 E_c I_c}{{L_c}^2} \qquad (7)$$

D_{sym}, D_{anti} represent the effective natural circular frequencies of the stayed column, and is calculated by comparison to the nondimensional quantities Ψ_{sym} and Ψ_{anti} where

$$\frac{2K_s \sin^2\alpha}{B_c} = \frac{{D_{sym}}^3}{D_{sym} - \tan D_{sym}} \qquad (8)$$

$$\frac{B_c}{\sin^2\alpha}\left(\frac{\cos^2\alpha}{3B_a}+\frac{1}{2K_s}\right) = \frac{D_{anti}-\tan D_{anti}}{{D_{anti}}^2\tan D_{anti}} \quad (9)$$

and

$$\Psi_{sym} = \frac{2K_s\sin^2\theta}{B_c} \quad (10)$$

$$\Psi_{anti} = \frac{1}{B_c}\left(\frac{1}{3B_a\tan^2\alpha}+\frac{1}{2K_s\sin^2\alpha}\right)^{-1} \quad (11)$$

where bending stiffness of the column and crossarms B_c and B_a are derived from

$$B_c = \frac{8E_cI_c}{{L_c}^3} \quad (12)$$

$$B_a = \frac{E_aI_a}{{L_a}^3} \quad (13)$$

As stated

$$N^c_{max} = \min\left(N^c_{max,sym}, N^c_{max,anti}\right) \quad (14)$$

This defines the optimum theoretical stay tension where

$$T_{opt} = N^c_{max}C_{11} \quad (15)$$

The eigenvalue critical buckling load is calculated differently for the three zones of stay pre tension shown in Fig. 3 [7] where

$$N^C_{sym,z1} = N_{cr} \quad (16)$$

$$N^C_{sym,z2} = \left(\frac{N^c_{max}-N_{cr}}{T_{opt}-T_{min,sym}}\right)T \quad (17)$$

$$N^C_{sym,z3} = (N^c_{max}-2T\cos(\alpha))C_{22} \quad (18)$$

$$N^C_{anti,z1} = 4N_{cr} \quad (19)$$

$$N^C_{anti,z2} = \left(\frac{N^c_{max}-4N_{cr}}{T_{opt}-T_{min,anti}}\right)T \quad (20)$$

$$N^C_{anti,z3} = (N^c_{max}-2T\cos(\alpha))C_{22} \quad (21)$$

The variable C_{22} used to define the critical load in zone 3 is defined by

$$C_{22} = \frac{\cos^2(\alpha)}{K_c\left[\frac{1}{K_s}+\frac{2(\sin^2\alpha)}{K_a}\right]}+1 \quad (22)$$

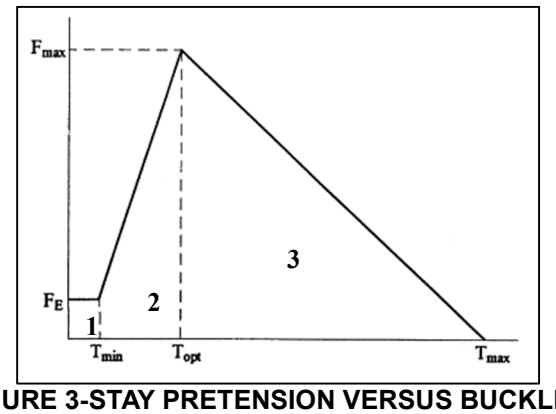

FIGURE 3-STAY PRETENSION VERSUS BUCKLING LOAD [7]

Column imperfection is introduced as a contributing factor to calculate the normalised maximum load carrying capacity (N_{max}/N^c) of a prestressed stayed column. Zone 2 is split into two equations at $T \approx 0.4T_{opt}$ as at this point there is a transition from stable to unstable post-buckling behaviour.

$$\left(\frac{N_{max}}{N^c}\right)_{sym,z2a} = \left[\frac{1-\left(\frac{N_{max}}{N^c}\right)_{sym,z1}}{0.4T_{opt}-T_{min}}\right](T-T_{min}) + \left(\frac{N_{max}}{N^c}\right)_{sym,z1} \quad (23)$$

$$\left(\frac{N_{max}}{N^c}\right)_{sym,z2b} = \left[\frac{\left(\frac{N_{max}}{N^c}\right)_{Topt}-1}{0.6T_{opt}}\right](T-0.4T_{opt}) + 1 \quad (24)$$

$$\left(\frac{N_{max}}{N^c}\right)_{sym,z3} = \left[\frac{\left(\frac{N_{max}}{N^c}\right)_{3Topt}-\left(\frac{N_{max}}{N^c}\right)_{Topt}}{2T_{opt}}\right](T - T_{opt}) + \left(\frac{N_{max}}{N^c}\right)_{Topt} \quad (25)$$

$$\left(\frac{N_{max}}{N^c}\right)_{anti,z2} = \left[\frac{\left(\frac{N_{max}}{N^c}\right)_{Topt}-\left(\frac{N_{max}}{N^c}\right)_{anti,z1}}{T_{opt}-T_{min}}\right](T - T_{min}) + \left(\frac{N_{max}}{N^c}\right)_{anti,z1} \quad (26)$$

$$\left(\frac{N_{max}}{N^c}\right)_{anti,z3} = \left[\frac{\left(\frac{N_{max}}{N^c}\right)_{3Topt}-\left(\frac{N_{max}}{N^c}\right)_{Topt}}{2T_{opt}}\right](T - T_{opt}) + \left(\frac{N_{max}}{N^c}\right)_{Topt} \quad (27)$$

Parameters $\left(\frac{N_{max}}{N^c}\right)_{sym,z1}$, $\left(\frac{N_{max}}{N^c}\right)_{anti,z1}$, $\left(\frac{N_{max}}{N^c}\right)_{Topt}$ and $\left(\frac{N_{max}}{N^c}\right)_{3Topt}$ are given in Tables A1 and A2 of the appendix as functions of imperfection level [8].

The above equations are for a 2D planar system. When considering a 3D system, C_{22} must be adapted

$$C_{22,3D} = \frac{2\cos^2(\alpha)}{K_c\left[\frac{1}{K_s} + \frac{2(\sin^2\alpha)}{K_a}\right]} + 1 \qquad (28)$$

Also, the initial prestress component in the perpendicular direction (T_2) is found from the main column load carrying capacity using the angle between the main column and the stay in the perpendicular direction (θ_2) and the maximum load carrying capacity of the planar stayed column (N_{max}):

$$N_{max,3D} = N_{max} - 2T_2\cos\alpha_2 \qquad (29)$$

Considering the buckling analysis of prestressed stayed column, symmetric and antisymmetric buckling modes occur at different crossarm to length ratios, where

$$(2L_a/L_c)_{sym} = [0.05, 0.175] \qquad (30)$$

$$(2L_a/L_c)_{anti} > 0.175 \qquad (31)$$

Numerical modelling has generally been completed by Finite Element Analysis (FEA) of the prestressed stayed column system [4, 5, 7, 9]. The column and crossarms are modelled as elastic beams and the stays are modelled as trusses or link elements that are only able to be stressed in tension, thus simulating a cable and not a rigid member.

de Araujo et al. [7] concluded that columns using cable stays with an imperfection L/1500 presented an increase in the column load capacity of 160% when compared to equivalent solutions without stays.

Chan et al. [10] have also found that the buckling capacity of a column will be increased significantly by using pre-tensioned stays. In this study it was also found that initial imperfection also had a significant effect on buckling load.

Saito and Wadee [5] have found that when interactive buckling is considered, increasing the prestress above the theoretical optimum will increase the maximum load capacity and the system less imperfection sensitive.

It should be noted that all of the literature found regarding prestressed stayed column analysis has modelled the boundary conditions for the main column as pinned/pinned, meaning that the base of the column has zero degrees of freedom in displacement and one degree of freedom in rotation, and the top has a degree of freedom of displacement about the vertical axis and one degree of freedom in rotation. For the application of a prestressed stayed column as a wind turbine tower the boundary condition would be fixed/free, which does not have the same base conditions as a pinned/pinned tower. No literature can be found on finite element analysis of prestressed stayed columns for fixed/free end conditions.

PROPOSED STAYED COLUMN DESIGN

The previously analysed designs have involved stayed columns with external crossarms. A new design of stayed column that has internal crossarms can be seen in Figure 4 with corresponding dimensions. No source material can be found for the structural analysis for this design of prestressed stayed column.

This design applies lateral force on the column in the opposite direction to that applied by the designs of stayed column reviewed so far. However, it is possible to apply a similar lateral load to external crossarm systems by linking the stays to the crossarms in a crossed configuration. This case will also be analysed. The two configurations will be referred to as Configuration A and Configuration B. Configurations A and B will each consist of eight stays that have equal pretension.

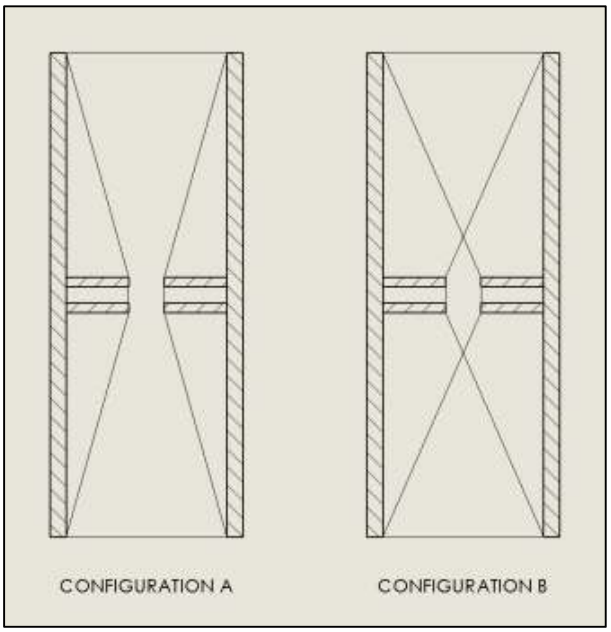

FIGURE 4- INTERNALLY STAYED TOWER DESIGN CONCEPT

The testing will encompass three column analyses, incorporating subcases where relevant (Table 1). Subcase **a** is defined in Table 2, and subcase **b** is defined in Table 3. For Subcase **a** it can be seen that the maximum tension through the stays is 75kN, which gives a stress of 9.55MPa. Given that the standard yield stress of steel is 250MPa this applied stress is feasible, and gives a safety factor of 26.28.

Using the data for the 5MW wind turbine tower and the 5MW wind turbine head assembly load (see Table 4), the parameters for the system are defined as in Table 5. These

values incorporate the column thickness for varied pretension (0.06m) and the pretension for varied column thickness (35kN).

TABLE 1- TEST CASES

Case	Model	Subcase	Procedure
1	Simple Column	b	vary column thickness
2	Internally Stayed Column Configuration A	a	vary pretension
		b	vary column thickness
3	Internally Stayed Column Configuration B	a	vary pretension
		b	vary column thickness

TABLE 2-TEST SUBCASES-a

Subcase	Tension	Subcase	Tension
1	0.1kN	9	40kN
2	5kN	10	45kN
3	10kN	11	50kN
4	15kN	23	55kN
5	20kN	13	60kN
6	25kN	14	65kN
7	30kN	15	70kN
8	35kN	16	75kN

TABLE 3- TEST SUBCASES-b

Case	Assembly Model	Column Thickness
1	Assy_1	0.04m
2	Assy_2	0.05m
3	Assy_3	0.06m
4	Assy_4	0.07m
5	Assy_5	0.08m

TABLE 4-5MW NREL WIND TURBINE TOWER DIMENSION

Hub Height	100m
Top Diameter	3.8m
Bottom Diameter	4.5m
Plate Thickness	0.068m

TABLE 5-TEST PARAMETERS

Column Length (Lc)	100m
Column Thickness (Tc)	0.06m
Column Radius (Rc)	2.25m
Crossarm Length (La)	1.765m
Crossarm Thickness (Ta)	0.05m
Crossarm Radius (Ra)	0.375m
Stay Radius (Rs)	0.05m
Load	3.5MN
Load Eccentricity	0.45m
Cable Tension	35kN

The load eccentricity was chosen at a fifth of the column radius because this would compensate for the lack of geometrical imperfections and allow the column to deflect. The magnitude of load applied on the column is not expected to induce buckling, so incorporating this eccentricity should yield enough deflection to gain substantial results that are more than negligible, where the critical buckling load for the non-stayed column of these dimensions is 101.6MN.

Opposite crossarms have a 0.85m clearance, which results in a 0.05m square clearance between adjacent crossarm end points. This is to allow for crossarm movement caused by column deflection so that there is no interference, and is the same for both configurations of the internally stayed column.

The material used for the column and crossarms is standard structural steel defined by ANSYS Engineering Data, which has a Young's Modulus of 200GPa and a Poisson's Ratio of 0.3. The material for the stays is defined in the prestress code, and is modelled on steel with a Young's Modulus of 200GPa and a Poisson's Ratio of 0.3.

ANALYSIS AND DISCUSSION

The analysis is performed using ANSYS Workbench, and utilises the ANSYS Mechanical FEA solver. Figure 5 shows a typical deflection solution.

Figures 6 and 7 show the reduction in normalised column deflection ($1-\delta^*$) plotted against stay pretension to applied load ratio (T^*) for Configurations A and B. From these graphs the minimum effectual and optimum stay tension to load ratios (T^*_{MIN}, T^*_{OPT}) for each configuration of internally stayed prestressed column can be estimated with good accuracy. These are the points at which the steep change in reduced normalised column deflection begins and ends. For finding T^*_{MIN} and T^*_{OPT} Figure 7 is more accurate, as less noise from lower normalised load curves is present.

It can be seen that the normalised column deflection for Configuration A is lower than for Configuration B for any given case above the minimum effectual stay tension to load ratio of Configuration A, which means that Configuration A has the greater resistance to deflection under load.

The anomalous curves in Figure 6 show the 0.05 normalised applied load curves that have a secondary increase in the reduction of normalised column deflection after a stay tension to load ratios of around 0.22-0.23. Increased stay tension/applied load ratios should be analysed in future work.

The maximum reduction in normalised column deflection indicates the maximum percentage of deflection reduced as a result of the pretensioned stays. It is found that T^*_{OPT} for Configuration A has a reduction in normalised deflection 120% more than T^*_{OPT} for Configuration B. However the maximum reduction of normalised deflection for each configuration is very small, with maximum values of 0.011 for Configuration A and 0.005 for Configuration B according to Figure 7.

Figure 7 can be compared to Figure 3 for the maximum load capacity vs. stay pretension, as reduction in column deflection is proportional to critical load capacity. Using the current theory described at the beginning of the paper, the maximum

load capacity and optimum stay pretension of a pinned/pinned externally stayed prestressed column of the same dimensions were found. Dividing the calculated optimum pretension by the maximum load capacity yields a result of 0.019. The approximate corresponding value for Configuration A of the internally stayed column is 0.012, and for Configuration B it is 0.011.

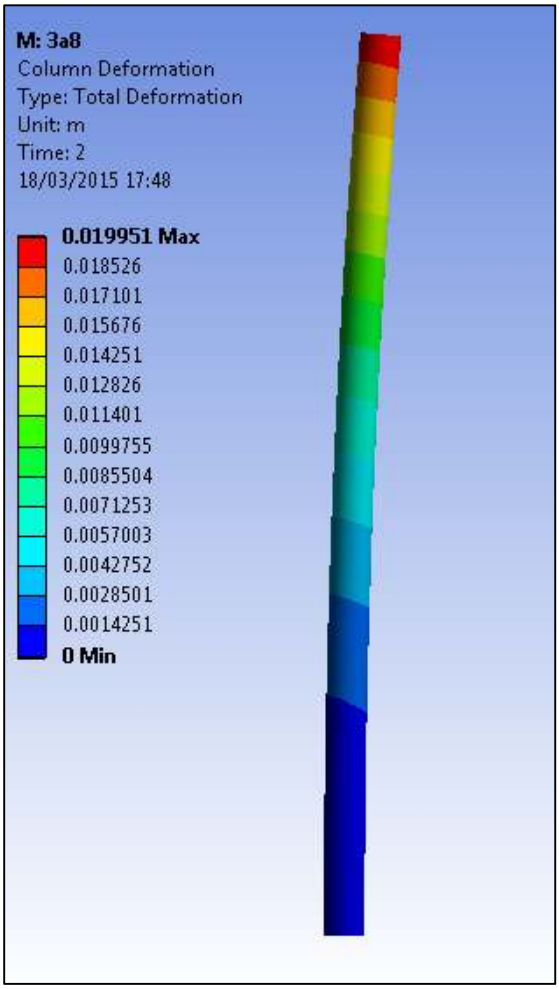

FIGURE 5-TYPICAL DEFLECTION SOLUTION

Figure 8 shows the plot of reduction in normalised column deflection vs. normalised column thickness. For Configuration A of the internally stayed column, the maximum reduction in normalised column deflection range occurs at a normalised column thickness of 0.75. This means that after this point the system is converging, so at 0.75 normalised column thickness the deflection is most affected by load. For Configuration B the maximum normalised column deflection range occurs at a normalised column thickness of 0.875.

It can be seen that for all cases normalised column deflection is greatly reduced with increasing normalised column thickness. Also, at a constant normalised column thickness, an increase in normalise load decreases the normalised column deflection. It is observed that the higher the normalised load, the greater the reduction in column deflection for any analysed normalised column thickness as seen in Figure 9 and by analysing the gathered data.

The ranges of the normalised column deflection at each normalised column thickness for 0.05 to 1 normalised loads are shown in Figure 9. This means that a change in load affects the column deflection of Configuration A the most.

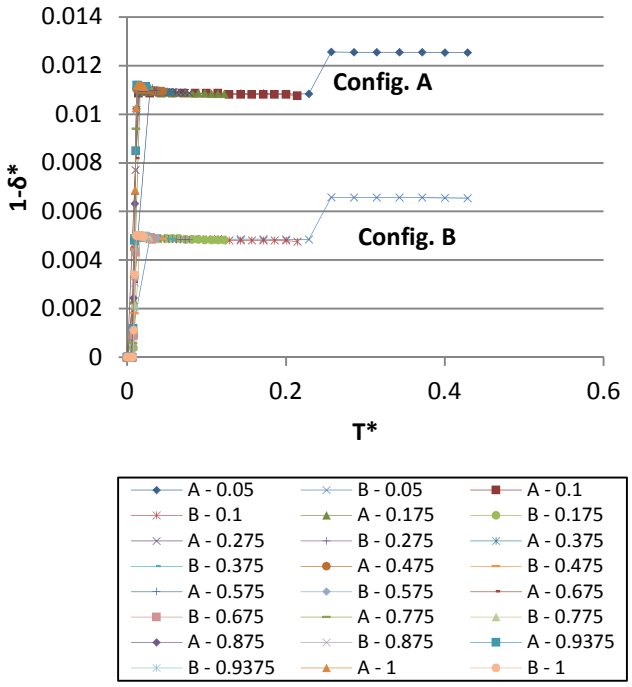

FIGURE 6-EFFECT OF STAY TENSION ON REDUCTION IN NORMALISED DEFLECTION

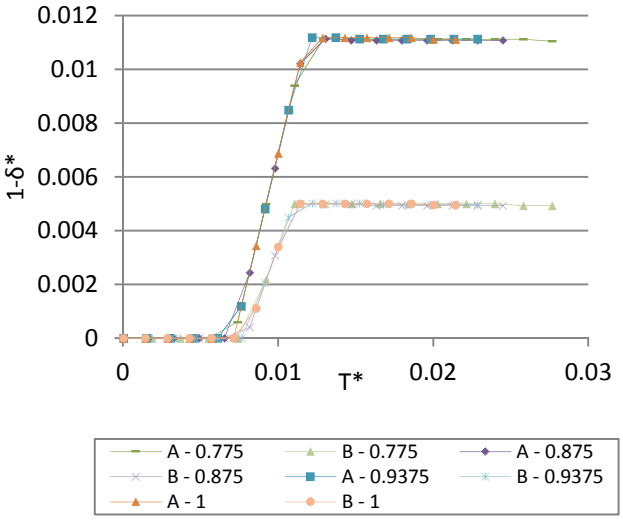

FIGURE 7- EFFECT OF STAY TENSION ON REDUCTION IN NORMALISED DEFLECTION (REFINED)

CONCLUSION

From these results, the following conclusions can be derived:

1. Both Configuration A and Configuration B of the internally stayed column design increase the stiffness of a column, and Configuration A increases the stiffness more than Configuration B.
2. Internally stayed systems at fixed/free end constraints have lower optimum stay tension to load ratio than the same sized system with external crossarms at pinned/pinned end constraints.
3. Increasing column thickness decreases column deflection for applied axial eccentric load. This is shown to a greater extent by Configuration A of the internally stayed column than Configuration B, which is again more than a non-stayed column.
4. A column of thickness in Configuration A experiences a greater change in decreased deflection than a column in Configuration B over increasing normalised applied load, making it more adaptable to higher load cases.
5. The difficulties of using internally stayed column designs of the analysed designs as wind turbine towers would greatly outweigh the benefits, as the maximum normalised deflection reduction is only 1.1%. It would be much more effective to slightly increase the thickness of the column, as thickness has a greater bearing on the deflection of the column than adding pretensioned stays.

A possible reason for the finding that Configuration A performs better under loading than Configuration B is that the stresses imparted on the column from the direction of pretension applied on the crossarms are influential. From Figure 10 it can be seen that Configuration B exhibits much higher localised stresses around the crossarm contact locations. Also the deformed shape of the column is more rounded in Configuration A, and the general axial stress is more constant and of greater magnitude, where in Configuration B the axial stresses are low and varied. This can be seen at the element faces where the section is cut, and would give Configuration A greater stress stiffening.

It should be noted that the crossarm to column length ratio in this study is less than the minimum for buckling failure mode calculation in the current theory for prestressed stayed columns.

There is a large scope for future work for the analysis of internally stayed prestressed columns, such as critical buckling load analysis. Also, many system parameters could be made variable for tests to determine their contribution to the stiffness of the internally stayed column, such as stay diameter, column end condition, crossarm length as a proportion of column internal diameter, material usage, etc. Different configurations could also be analysed, which incorporate multiple crossarms, or crossarms located a different heights.

For further analysis into internally stayed column usage as a wind turbine tower, more testing should be carried out over a more wide range of load cases as defined in Figure 1.

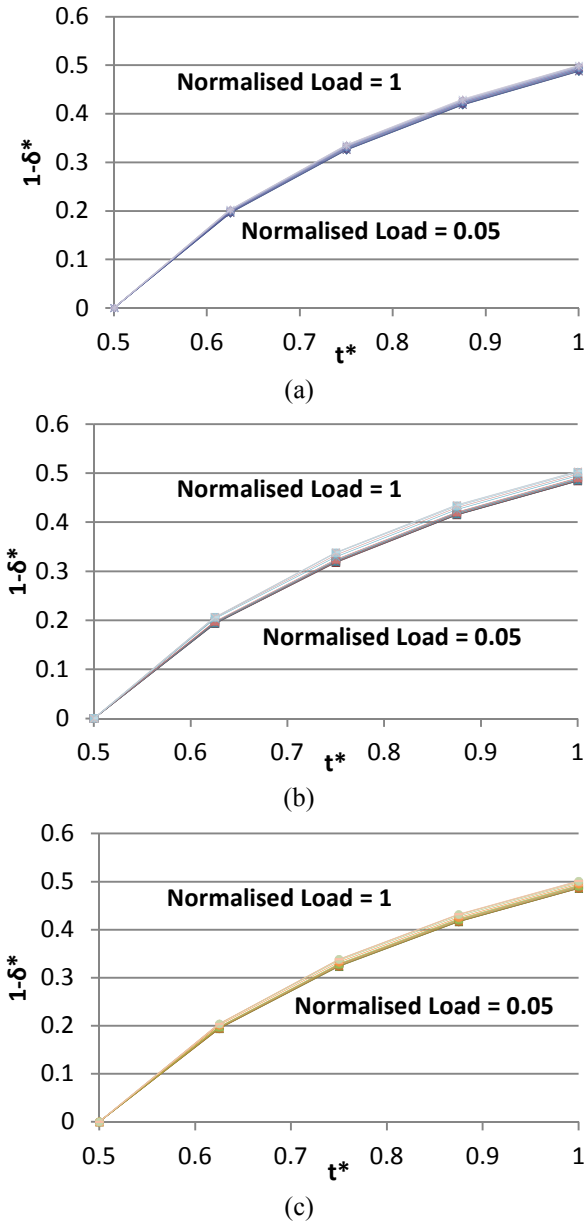

FIGURE 8-EFFECT OF COLUMN THICKNESS ON REDUCTION IN NORMALISED DEFLECTION, TEST CASES: 1b (a), 2b (b) and 3b (c)

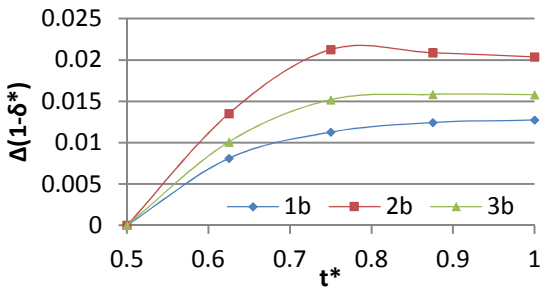

FIGURE 9-RANGE OF REDUCTION IN NORMALISED DEFLECTION, TEST CASES: 1b, 2b and 3b

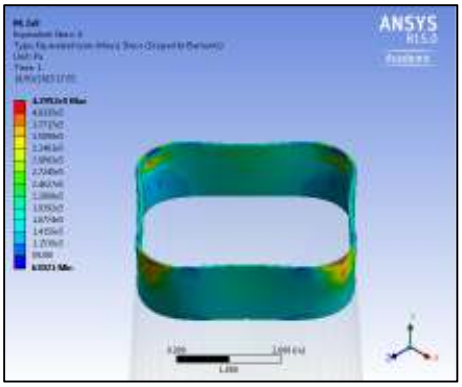

(a) CONFIGURATION A

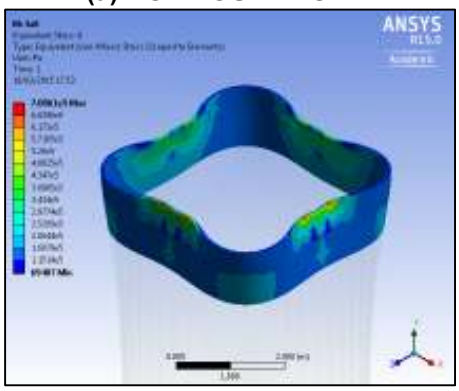

(b) CONFIGURATION B

FIGURE 10-MID-COLUMN STRESS AT 35 kN STAY PRETENSION

NOMENCLATURE

A	Cross-sectional Area	m^2
B	Bending Stiffness	Nm^{-3}
C_{11}	Non-dimensional Value	
C_{22}	Non-dimensional Value	
D	Effective Natural Circular Frequencies	Hz
E	Young's Modulus	Pa
I	Second Moment of Area	m^4
K	Stiffness	Nm^{-1}
L	Length (m)	m
N^c_{max}	Maximum Critical Buckling Load for Stayed Column	N
N_{cr}	Critical Buckling Load for Simple Column	N
t^*	Normalised Column Thickness	
T^*_{MIN}	Minimum Effectual Stay Pretension to Load Ratio	
T^*_{OPT}	Optimum Stay Pretension to Load Ratio	
T_{min}	Minimum Effectual Stay Tension	N
T_{opt}	Optimum Theoretical Stay Tension	N
δ^*	Normalised Column Deflection	
α	Stay Angle	rad
Ψ	Non-dimensional Value	

REFERENCES

[1] Nicholson, JC, Design of wind turbine tower and foundation systems: optimization approach, MS Thesis, Department of Civil and Environmental Engineering, University of Iowa, 2011.IEC 61400-1, International Standard, "Wind Turbines – Part1: Design Requirements", Third Edition, 05-08

[2] Önder UMUT, Bülent AKBAS, Jay SHEN, Design Issues of Wind Turbine Towers, Proceedings of the 8th International Conference on Structural Dynamics, EURODYN 2011, Leuven, Belgium, 4-6 July 2011, G. De Roeck, G. Degrande, G. Lombaert, G. Müller (eds.), ISBN 978-90-760-1931-4

[3] International Transport Forum, Permissable Maximum Dimensions of Trucks in Europe, 15 Jan 2013

[4] Daisuke Saito, M. Ahmer Wadee, Post-buckling behaviour of prestressed steel stayed columns, Engineering Structures, Volume 30, Issue 5, May 2008, Pages 1224-1239, ISSN 0141-0296

[5] Daisuke Saito, M. Ahmer Wadee, Numerical studies of interactive buckling in prestressed steel stayed columns, Engineering Structures, Volume 31, Issue 2, February 2009, Pages 432-443, ISSN 0141-0296

[6] M. Ahmer Wadee, Leroy Gardner, A. Israel Osofero, "Design of prestressed stayed columns", Journal of Constructional Steel Research, Volume 80, January 2013, Pages 287-298, ISSN 0143-974X

[7] R.R. de Araujo, S.A.L. de Andrade, P.C.G.da.S. Vellasco, J.G.S. da Silva, L.R.O. de Lima, Experimental and numerical assessment of stayed steel columns, Journal of Constructional Steel Research, Volume 64, Issue 9, September 2008, Pages 1020-1029, ISSN 0143-974X

[8] A. Maheri, A.I. Osofero, M. Corradi, "The Effect of Column Length and Size on the Maximum Achievable Load Carrying Capacity of Prestressed Stayed Columns", in B.H.V. Topping, P. Iványi, (Editors), "Proceedings of the Twelfth International Conference on Computational Structures Technology", Civil-Comp Press, Stirlingshire, UK, Paper 7, 2014. doi:10.4203/ccp.106.7

[9] Osofero, A. Israel, M. Ahmer Wadee, and Leroy Gardner. "Numerical studies on the buckling resistance of prestressed stayed columns." Advances in Structural Engineering 16.3 (2013): 487-498.

[10] Siu-Lai Chan, Gan-ping Shu, Zhi-tao Lü, Stability analysis and parametric study of pre-stressed stayed columns, Engineering Structures, Volume 24, Issue 1, January 2002, Pages 115-124, ISSN 0141-0296

[11] J. Jonkman, S. Butterfield, W. Musial, and G. Scott, "Definition of a 5-MW Reference Wind Turbine for Offshore System Development", National Renewable Energy Laboratory, Technical Report NREL/TP-500-38060 February 2009

ANNEX A

EIGENMODE BUCKLING LOAD RATIO

TABLE A1- SYMMETRIC EIGENMODE BUCKLING LOAD RATIO

Imperfection Level	$\left(\frac{N_{max}}{N^c}\right)_{sym,z1}$	$\left(\frac{N_{max}}{N^c}\right)_{Topt}$	$\left(\frac{N_{max}}{N^c}\right)_{3Topt}$
$\frac{L_c}{1000}$	$19\left(\frac{2L_a}{L_c}\right)+0.10$	$14.0\left(\frac{2L_a}{L_c}\right)^2-3.10\left(\frac{2L_a}{L_c}\right)+0.75$	$1.0-1.2\left(\frac{2L_a}{L_c}\right)$
$\frac{L_c}{400}$	$17\left(\frac{2L_a}{L_c}\right)+0.13$	$58.0\left(\frac{2L_a}{L_c}\right)^2-14.1\left(\frac{2L_a}{L_c}\right)+1.16$	$0.84-1.2\left(\frac{2L_a}{L_c}\right)$
$\frac{L_c}{200}$	$13.5\left(\frac{2L_a}{L_c}\right)+0.28$	$0.71-3.0\left(\frac{2L_a}{L_c}\right)$	$0.72-1.4\left(\frac{2L_a}{L_c}\right)$

TABLE A2- ANTISYMMETRIC EIGENMODE BUCKLING LOAD RATIO

Imperfection Level	$\left(\frac{N_{max}}{N^c}\right)_{anti,z1}$	$\left(\frac{N_{max}}{N^c}\right)_{Topt}$	$\left(\frac{N_{max}}{N^c}\right)_{3Topt}$
$\frac{L_c}{1000}$	$1.0\left(\frac{2L_a}{L_c}\right)+0.8$	$1.5\left(\frac{2L_a}{L_c}\right)+0.25$	0.74
$\frac{L_c}{400}$	$0.80\left(\frac{2L_a}{L_c}\right)+0.63$	$0.70\left(\frac{2L_a}{L_c}\right)+0.33$	0.58
$\frac{L_c}{200}$	$0.70\left(\frac{2L_a}{L_c}\right)+0.44$	$0.60\left(\frac{2L_a}{L_c}\right)+0.20$	0.43